Cellular Physiology and Biochemistry

Cell Physiol Biochem 2018;50:411-425
DOI: 10.1159/000494153
Published online: 11 October 2018
Accepted: 2 October 2018

Original Paper

Hypermethylation of miR-338-3p and Impact of its Suppression on Cell Metastasis Through N-Cadherin Accumulation at the Cell -Cell Junction and Degradation of MMP in Gastric Cancer

Bo Guo[a] Jing Zhang[b] Qian Li[a] Zhenghao Zhao[c] Wenjing Wang[d] Kaiyue Zhou[e] Xiaofei Wang[g] Dongdong Tong[a] Lingyu Zhao[a] Juan Yang[a] Chen Huang[a,f,g]

[a]Department of Cell Biology and Genetics, School of Basic Medical Sciences, Xi'an Jiaotong University Health Science Center, Xi'an, [b]Department of Clinical Medicine, Medical College of Yan'an University, Yan'an, [c]The ART Center, Northwest Women's and Children's Hospital, Xi'an, [d]Department of Hepatobiliary Surgery, First Affiliated Hospital, Xi'an Jiaotong University, Xi'an, China, [e]Program in Plant Biology and Conservation, Biological Sciences, Weinberg College of Arts and Sciences, Northwestern University, IL, USA, [f]Key Laboratory of Shaanxi Province for Craniofacial Precision Medicine Research, College of Stomatology, Xi'an Jiaotong University, Xi'an, [g]Key Laboratory of Environment and Genes Related to Diseases, Xi'an Jiaotong University, Ministry of Education of China, Xi'an, China

Key Words
miR-338-3p • Gastric cancer • Metastasis • Rab14-N-cadherin • Hhat-MMP signaling

Abstract
Background/Aims: MicroRNAs (miRNAs) have been well studied in human carcinogenesis and cancer progression. Our previous study showed the down-regulation of miR-338-3p expression in human gastric cancer (GC). However, the reasons of this dysregulation remain largely unclear. ***Methods:*** Bisulfite sequence analysis was performed to explore the methylation status of the promoter region of miR-338-3p. Cell wound-healing and transwell assays were performed to examine the capacity of cell migration and cell interaction. A dual-luciferase reporter was used to validate the bioinformatics-predicted target gene of miR-338-3p. Western blotting, RNA interference, and immunofluorescence (IF) were used to evaluate the expression of MMPs and the location of N-cadherin to determine the mechanism underlying miR-338-3p-induced anti-tumor effects. ***Results:*** miR-338-3p was epigenetically silenced, and this loss of expression was significantly correlated with the Borrmann Stage in GC. Restoring miR-338-3p expression in BGC-823 cells inhibited cell migration and invasion.

B. Guo, J. Zhang and Q. Li contributed equally to this work.

Dr. Bo Guo
and Dr. Chen Huang
Department of Cell Biology and Genetics, School of Basic Medical Sciences
Xi'an, Shaanxi (China)
E-Mail bo_guo@xjtu.edu.cn; hchen@mail.xjtu.edu.cn

Moreover, Ras-related protein (Rab-14) and Hedgehog acyltransferase (Hhat) were identified as direct targets of miR-338-3p. Both enforced expression of miR-338-3p and small interfering RNA induced Rab14-mediated accumulation of N-cadherin in the cell -cell junctions or Hhat-associated matrix metalloproteinase (MMP) degradation, which may underline the metastasis defects caused by loss of miR-338-3p in GC. ***Conclusion:*** These data indicate that miR-338-3p functions as a tumor suppressor in GC, and that the hypermethylation status of its CpG island might be a novel potential strategy for treating GC.

Introduction

Gastric cancer (GC) is one of the most frequent malignancies and is a leading cause of cancer-related death worldwide [1]. Aberrant expressions of microRNAs (miRNAs) that lead to tumorigenesis or have tumor-suppressing effects have been well studied in GC progression over the past decade [2]. Moreover, recent studies have identified that epigenetic alteration (i.e., DNA methylation) could play a critical role in the regulation of miRNA expression in GC. For example, hypermethylation-silenced miR-129 expression has been found to be associated with poor clinical outcome in GC. Moreover, restoration of miR-129 decreases the expression of its target gene, SRY-related high-mobility group box 4 (*SOX4*) and reduces proliferation of cancer cells [3, 4]. In another study, miR-10b was found to be silenced in GC cells due to its heavily methylated promoter CpGs, whereas transfection with precursor miR-10b into GC cells dramatically decreased the mRNA and protein of the target gene, microtubule-associated protein RP/EB family member 1 (*MAPRE1*), and resulted in a significant decrease in colony formation and cell growth rates [5]. Therefore, DNA methylation plays key roles in controlling the expression of tumor-suppressive miRNAs in the developmental stages of gastric tumors. Our previous studies have demonstrated that miR-338-3p is significantly down-regulated in GC and that could suppress GC progression through the PTEN-AKT axis by targeting P-Rex2a both *in vivo* and *in vitro* [6]. However, the mechanisms of miR-338-3p dysregulation in GC remain largely unclear.

The high mortality rate of GC is mainly due to the development of metastases at advanced stages, which means the tumors can spread throughout the stomach and to other organs. Many studies have investigated the genes that drive metastasis. Recent studies have also reported that miRNAs could act as activators or inhibitors by targeting multiple signaling pathways involved in metastasis [7-9]. For instance, miR-218 was identified as a tumor-suppressing miRNA, which can negatively regulate roundabout guidance receptor 1 (*ROBO1*), one of the several slit receptors, thus enhancing Slit/Robo1 signaling when suppressed. Restoration of miR-218 expression inhibited invasion and metastasis of GC both *in vitro* and *in vivo* [10]. On the contrary, miR-107 and miR-199a were found to be frequently up-regulated in metastatic GC tissues. Subsequent research characterized *DICER1* and mitogen-activated protein kinase 11 (*MAP3K11*) as direct targets of miR-107 [11] and miR-199a [12], respectively. These results suggest that miR-107 and miR-199a are oncogenes that promote GC metastasis and are significantly correlated with clinical progression. In the present study, we discovered that the downregulated expression of miR-338-3p is correlated with the Borrmann Stage, an independent prognostic factor of survival that represents the metastasis ability of gastric cancer cells [13].

It is well known that miRNAs regulate hundreds of potential genes by binding to the 3'-untranslated region (UTR) of target mRNAs, and we identified Ras-related protein (Rab-14) and Hedgehog acyltransferase (HHAT) as two potential targets of miR-338-3p by using a gene target prediction database (i.e., miRanda, PicTar, and TargetScan). In this study, we provide evidence that Rab14-mediated N-cadherin accumulation at cell-cell junctional complexes and Hhat-regulated matrix metalloproteinase (MMP) signaling degradation may underlie the metastasis defect caused by miR-338-3p. In addition, we also found that the hypermethylation of CpGs in the promoter region of miR-338-3p is the main reason for miR-338-3p dysregulation in GC. The results reported here comprehensively demonstrated

dysregulation of miR-338-3p and its mechanisms and effects on the regulation of cell metastasis in GC, providing valuable insights for the development of more effective clinical therapies for GC in the future.

Materials and Methods

Clinical samples and cell culture

Human GC tissues and paired non-tumor gastric tissues (at least 5 cm away from the tumor edge) were obtained from patients who received surgical gastric resection at the First Affiliated Hospital of Xi'an Jiaotong University (from 2012 to 2014). Informed consent was obtained from each individual, and the study was approved by the Institute Research Ethics Committee at Cancer Center of Xi'an Jiaotong University. Human GC cells (BGC-823) and human embryonic kidney cells (HEK-293) were maintained in the Key Laboratory of Environment and Genes Related to Diseases at Xi'an Jiaotong University. Cells were cultured in Dulbecco's modified eagle's medium (PAA, Australia), supplemented with 10% fetal bovine serum (PAA, Australia) and 1% penicillin/streptomycin in a humidified atmosphere with 5% CO_2 at 37°C.

Treatment with 5-Aza-2'-deoxycytidine (5'-Aza-dC)

Cells were plated into 10-cm^2 dishes at the appropriate density. Each dish was treated with DNA methyltransferase inhibitor 5'-Aza-dC (Sigma-Aldrich, MO, USA), and DMSO was used as the control. Cells were continuously treated with 5'-Aza-dC (2.5 μM, 5 μM, 7.5 μM, 10 μM or 15 μM) for 3 days, and were, then harvested. Cell pellets were prepared for total RNA extraction using the Trizol protocol (Life Technologies, MD, USA) or Genomic DNA extraction for further study.

Genomic DNA extraction and bisulfite sequence analysis

Genomic DNA was prepared from cells after 5'-Aza-dC treatment, and bisulfite modification was performed by using EpiTect Bisulfite Kit (QIAGEN, CA, USA) according to the manufacturer's instructions. Bisulfite-treated DNAs were then used for PCR to obtain the two CpG islands (GRC37 version, UCSC) of the miR-338-3p promoter region. The purified PCR products were cloned into T vectors (Takara, Tokyo, Japan). Ten randomly selected clones were sequenced. The primers used for bisulfite-PCR are as follows: CpG island1 (F-5'*GGATAGGGTAGTGGGGTTTTTATTA*3', R-5'*CAAACTATACCCAACCCTAACTCAC*3') and CpG island2 (F-5'*GTTATGATTTGATATGGGTGGGTAG*3', R-5'*TCCCTATACCAACAAAAAAACTACTTC*3').

RNA extraction, cDNA synthesis, and quantitative real-time PCR

Total RNA was isolated from pre-prepared GC samples or BGC-823 cells with TRIzol reagent (Life Technologies, MD, USA), and cDNA was synthesized with PrimeScript RT Reagent Kit according to the manufacturer's protocol (TAKARA, Tokyo, Japan). Quantitative real-time PCR (qRT-PCR) was carried out using SYBR Green^{Ex} Taq™ II (TAKARA, Tokyo, Japan), and PCR-specific amplification reactions were conducted using the IQ5 Optical System (BIO-RAD, CA, USA). The relative expression of genes was calculated with the $2^{-(DDCt)}$ method. The primers used are listed as follows:

Rab14 (F-5'*GCAGATTTGGGATACAGCAGGG*3', R-5'*CAGTGTTTGGATTGGTGAGATTCC*3'),
HHAT (F-5'*GACGTGGCTCTGTTCTCTCC*3', R-5'*GGAGTAGGAGGTCGATGCAG*3'),
GAPDH (F-5'*TGAAGGTCGGAGTCAACGGATT*3', R-5'*CCTGGAAGATGGTGATGGGATT*3'),
miR-338-3p (F-5'*ATCCAGTGCGTGTCGTG*3', R-5'*TGCTTCCAGCATCAGTGAT*3', RT-5'*GTCGTATCCAGTGCGTG TCGTGGAGTCGGCAATTGCACTGGATACGACCAACAAA*3')
U6 (F-5'*GCTTCGGCAGCACATATACTAAAAT*3', R-5'*CGCTTCACGAATTTGCGTGTCAT*3',
RT-5'*CGCTTCACGAATTTGCGTGTCAT*3').

Plasmid construction and transfection

The construction of the miR-338-3p expression vector was performed as described previously [6]. For gene expression knockdown, shRNA (sh-control, sh-Rab14, and sh-Hhat) were purchased and verified by Shanghai Genechem Co. LTD. The plasmid DNAs were transfected with X-treme GENE HP DNA Transfection Reagent (Roche, CA, USA) according to the manufacturer's instructions. The transfection efficiency was

determined by qRT-PCR. The sequences are listed as follows: sh-Rab14 (5'*TGCAAGGAATCTCACCAAT*3'), sh-HHAT (5'*TCCATACCACCATCTCTTT*3'), and sh-control (5'*TTCTCCGAACGTGTCACGT*3').

Cell wound-healing assay

A wound-healing assay was performed to examine the capacity of cell migration and cell interaction. Briefly, once the cells had grown to 90% confluence in 12-well plates, a single scratch wound was generated with a 10 μl disposable pipette tip. The extent of wound closure was measured every 12 hours after wounding for 3 days.

Cell invasion assay

Cells in serum-free medium with epigenetic reagents or transfection treatment were added to the upper Matrigel Invasion Chamber (8 μm; BD, NJ, USA), and the bottom wells were filled with complete medium. The cells were allowed to migrate across the membrane for 48 hours. Following the incubation, cells were removed from the upper surface of the filter by scraping with a cotton swab. The invasive cells that adhered to the bottom of the membrane were stained with 1% crystal violet.

Dual-luciferase system

The 3'-UTR of Rab14 or Hhat containing miR-338-3p-binding sites was inserted between the Sac I and Xho I restriction sites of the pmirGLO Dual-Luciferase miRNA Target Expression Vector (Promega, WI, USA). Reporter gene assays were performed 48 hours after transfection using the dual-luciferase reporter assay system (Promega, WI, USA) according to the manufacturer's instructions. The normalized firefly luciferase activity (Firefly luciferase activity/Renilla luciferase activity) for each construct was compared with that of the pmirGLO vector control. All experiments were performed thrice.

Immunohistochemistry (IHC)

The GC samples were sectioned at a thickness of 4 μm. Sections were deparaffinized with xylene and hydrated using graded alcohol. Antigen retrieval and blocking were then performed, and slides were incubated with polyclonal rabbit anti-human RAB14 (1:200, #15662-1-AP, Proteintech, Wuhan, China) or HHAT (1:500, #98886, Abcam, MA, USA), followed by incubation with secondary antibodies. Detection was performed by 3, 3'-diaminobenzidine (DAB) and hematoxylin. The staining intensity was manually scored, and the sample was considered as highly expressed if the percentage of positive cells was >50% in five random fields.

Immunofluorescence (IF) microscopy

Cells were fixed with 4% paraformaldehyde in the presence of 0.02% Triton X-100 at room temperature for 20 min, followed by incubation in permeabilization / blocking solution (10% FBS, 0.5% Triton X-100 in PBS) at room temperature for 1 hour. The primary antibody N-cadherin (Cell Signal Technology, MA, USA) was diluted 1:500 in permeabilization / blocking solution and used to stain cells at 4°C overnight. The secondary antibody used was Alexa Fluor 647-conjugated goat anti-rabbit IgG (Molecular Probes, OR, USA). Cells were co-stained with the nucleic acid dye DAPI to visualize the nuclei.

Western blot analysis

Total proteins were extracted with RIPA lysis buffer (Wolsen, China) from cells harvested 48 hours after transfection and were separated by 10% SDS polyacrylamide gels. They were then electrophoretically transferred to a polyvinylidene difluoride membrane (Millipore, MD, USA). After the samples were incubated with primary antibodies at 4°C overnight and secondary antibodies for 2 hours at room temperature, they were visualized with enhanced chemiluminescence detection system (UVP, CA, USA). The primary antibodies for the differentially expressed gene used were as follows: rabbit polyclonal anti–RAB14 (1:500, #15662-1-AP, Proteintech, Wuhan, China), rabbit mAb anti-HHAT (1:1000, #98886, Abcam, MA, USA), rabbit mAb anti–E-Cadherin (1:1000, #3195, Cell Signal Technology, MA, USA), rabbit mAb anti-N-Cadherin (1:1000, #13116, Cell Signal Technology, MA, USA), rabbit mAb anti-MMP-2 (1:1000, #4022, Cell Signal Technology, MA, USA), rabbit mAb anti-MMP-9 (1:1000, #3852, Cell Signal Technology, MA, USA), and mouse monoclonal anti-GAPDH (1:1000, #8795, Sigma-Aldrich, MO, USA).

Statistical analysis

Each experiment was repeated at least three times independently. Data were presented as the mean ± SD and analyzed using the PASW Statistics 18 software (SPSS, USA). Differences between the two groups were calculated with the *Student'st*-test. A two-tailed value of $P<0.05$ was considered statistically significant.

Results

miR-338-3p is downregulated and correlated with the Bormann stage in GC

In our previous study, we found miR-338-3p was down-regulated in both GC tissues (53 paired samples) and cell lines (4 cancer cell lines) [6]. To further investigate the role of miR-338-3p from a clinical perspective, the association between miR-338-3p expression and clinicopathological factors was analyzed. Among the 20 paired informative samples, which contained the pathological files of depth of invasion (T), lymph node metastasis (N), hematogenous metastasis (M), Bormann stage, and differentiation, the decreased expression of miR-338-3p was found to be significantly associated with the Borrmann stage (Fig. 1A). Although we found that miR-338-3p could suppress cell proliferation and induce cell apoptosis, this finding led us to investigate the potential effect of miR-338-3p in GC on cell metastasis.

Epigenetic silencing of miR-338-3p in GC BGC-823 cells

As tumor-suppressor genes are frequently inactivated via an epigenetic mechanism, we investigated whether DNA demethylation regulated miR-338-3p expression. To assess the potential methylation status of the promoter region of miR-338-3p, we examined the methylation sites of CpG islands in 5'-Aza-dC treated cells and untreated cells by using bisulfite sequencing analysis with genomic DNA (Fig. 1B). The second CpG island in the miR-338-3p promoter region was found to be demethylated after 5'-Aza-dC treatment with a decrease from 97.4% to 71.5% (Fig. 1C and 1D), which was paralleled by the restoration of miR-338-3p expression, a result that has been previously described in a study that indicated that hyper-methylation is the main cause of miR-338-3p depression.

miR-338-3p suppresses metastasis of GC BGC-823 cells

Based on the association between miR-338-3p expression and clinical features, we investigated the effects of miR-338-3p on the metastasis features of migration and invasion in GC cells. By using the two major methods available (Transwell assay and wound-healing assay), transfection with miR-338-3p reduced the number of migrated cells by more than 50% (Fig. 2A). Moreover, compared with the control, miR-338-3p significantly blocked wound healing of BGC-823 cells (Fig. 2B).

Moreover, as mentioned above, the downregulation of miR-338-3p depends on epigenetic silencing, particularly DNA methylation. Treatment with 5'-Aza-dC restored the expression of miR-338-3p (Fig. 3A). Here, we also detected the effect on metastasis after 5'-Aza-dC treatment. As expected, 5'-Aza-dC treatment impeded cell metastasis (Fig. 3B and 3C), which was consistent with the increased expression of miR-338-3p. These results supported the hypothesis that miR-338-3p could contribute to suppression of metastasis in GC cells.

Rab14 is a direct target of miR-338-3p

We searched three bioinformatic databases (TargetScan, PicTar, and miRanda) to identify a large number of potential target genes of miR-338-3p. Among these candidates, Rab14 was selected for further analysis. To explore whether Rab14 is the direct target gene of miR-338-3p, a dual-luciferase reporter system including wild-type as well as mutant 3'-UTR of Rab14 was employed to examine the interaction between miR-338-3p and Rab14 (Fig. 4A). HEK293 cells were co-transfected with miR-338-3p or miR-control and with pmirGLO-Rab14-3'-UTR-wt or pmirGLO-Rab14-3'-UTR-mut. As shown in Fig. 4B, miR-338-3p clearly

A

Pathological Factors	Depth of invasion (T)				Lymph node metastasis (N)		Haematogenous metastasis (M)		Bormann Stage				Differentiation		
	T1	T2	T3	T4	Negative (N0)	Positive (N1-N3)	Negative (M0)	Positive (M1)	I	II	III	IV	Poor	Moderate	High
Patient Number (n=20)	2	4	3	11	2	18	17	3	2	5	7	6	12	6	2
P Value	0.159				0.238		0.699		**0.035***				0.236		

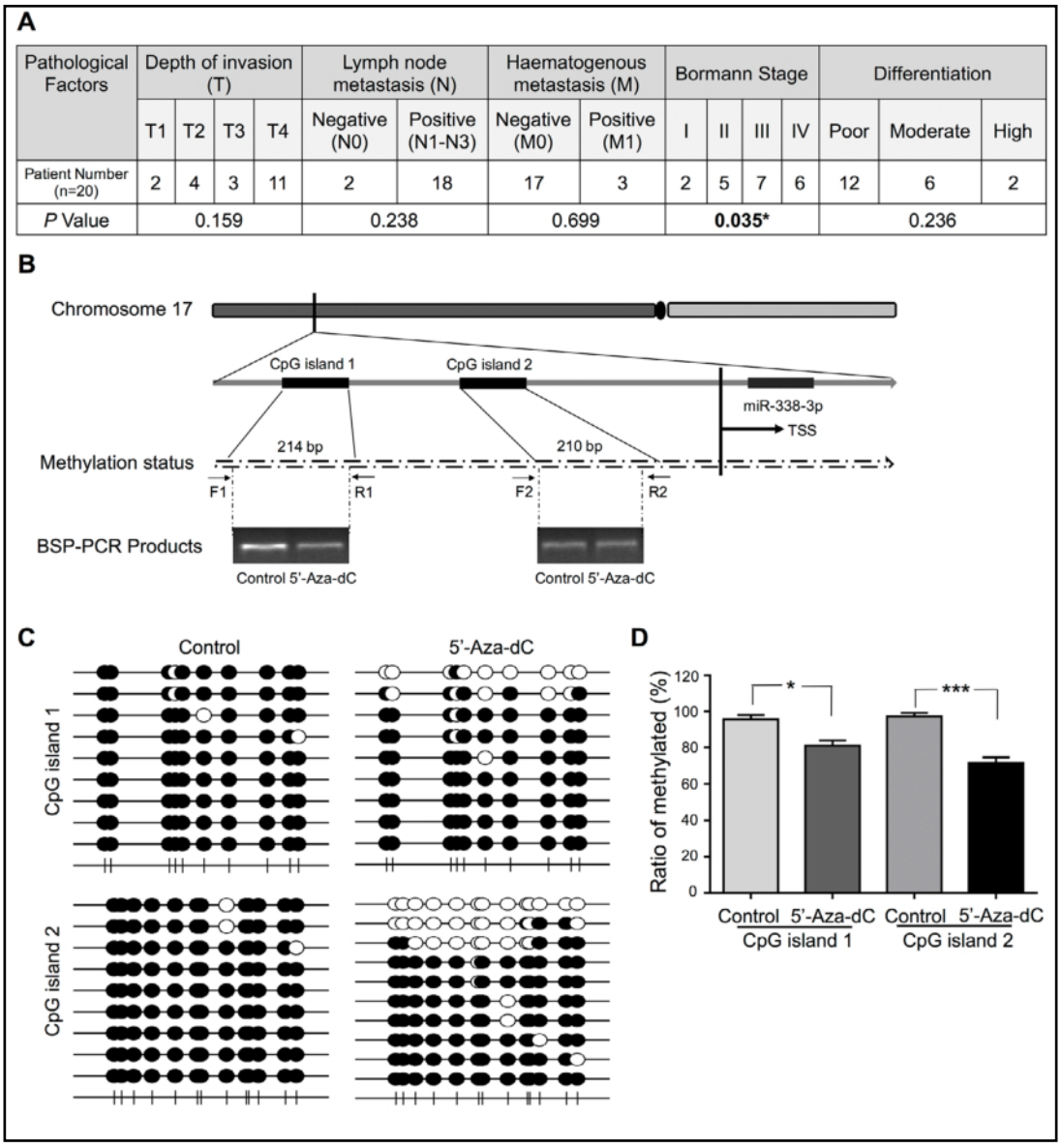

Fig. 1. The clinicopathologic association and epigenetic regulation of miR-338-3p depression in GC. (A) Relationship between miR-338-3p expression levels and clinicopathologic factors in 20 GC patients. (B) Schematic locations of CpG sites in the miR-338- 3p promoter region. Two CpG islands were obtained with BSP-PCR after treatment with 2.5 μM 5'-Aza-dC. (C/D) Bisulfite sequencing analysis of two CpG islands from ten randomly selected clones and summarized. (*P<0.05, ***P<0.001).

suppressed the firefly luciferase activity of pmirGLO-Rab14-3'-UTR-wt at 48 hours, while the mutant type was unaffected, which suggests that miR-338-3p directly targeted Rab14. Meanwhile, we also detected a decreased expression level of Rab14 after transfection with miR-338-3p, which shows that miR-338-3p was able to significantly suppress the expression of Rab14 on both mRNA and protein levels (Fig. 4C).

In our previously study, Rab14 was proven to be an oncogene in GC [14]. In this study, we also performed an IHC assay to confirm its over-expression in GC tissues (Fig. 4D). Furthermore, we silenced Rab14 in BGC-823 cells by RNA interference to confirm that Rab14 is involved in the anti-metastasis effects of miR-338-3p. Rab14 can be specifically knocked down by shRNA (Fig. 4E) at the transcription level. Moreover, silencing of Rab14 resulted in suppressed cell metastasis (Fig. 4F and G), which shows the same pattern as enforced miR-

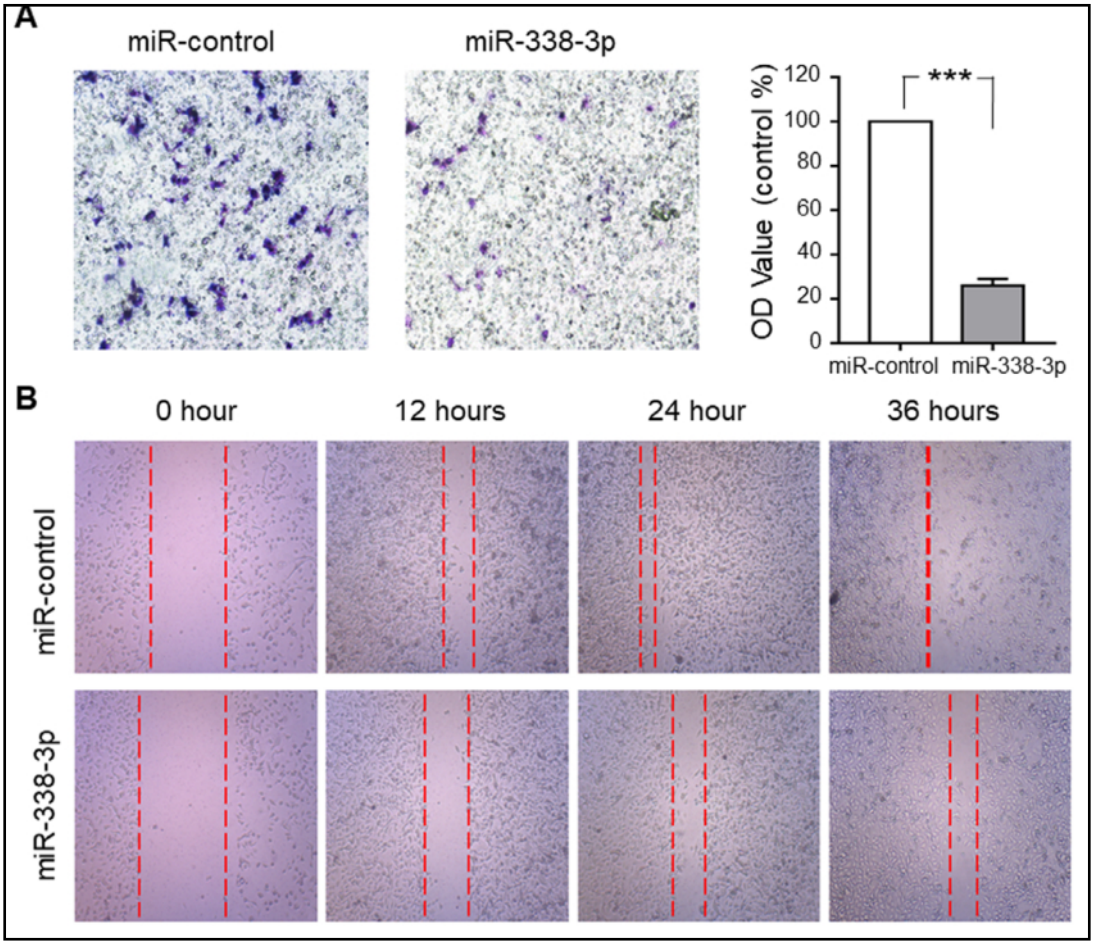

Fig. 2. Inhibition of GC cell invasion and migration after miR-338-3p transfection. (A) Tumor cell invasion assay. BGC-823 cells were transfected as described above and seeded into Transwell upper chambers for the cell invasion assay. Cells were transferred to the reverse side of the filter (left panel) and stained with 1% crystal violet for OD value measurements (right panel) (B) Wound healing assay. BGC-823 cells were transfected with miR-338-3p. Photographs were taken of these cells every 12 hours, and the remaining unhealed gap was marked. (***P<0.001).

338-3p. Taken together, these findings indicate that miR-338-3p suppresses cell metastasis by targeting Rab14.

N-Cadherin accumulation at cell-cell junctions in Rab14-silenced cells

Rab14 was found to play a crucial role in the regulation of membrane trafficking between the Golgi complex and the endosome [15]. Together with Rab GDP-GTP exchange factors FAM116, Rab14 also defined an endocytic recycling pathway needed for ADAM family protease ADAM10/Kuzbanian protease trafficking, as well as for regulation of cell-cell junctions by decreasing shedding of cell-surface N-cadherin [16]. Therefore, we also investigated the localization of N-cadherin in this study. A defined cell-cell junction staining of N-cadherin was clearly visible after transfection with miR-338-3p in comparison with the control cells (Fig. 5A). Moreover, RNA interference silencing of Rab14 also enriched the amount of N-cadherin at cell junctions (Fig. 5B). These results suggest that the elevated levels of N-cadherin at the cell-surface and increased cell-cell junction formation are the causes of the migration defect in Rab14-silenced cells, which is consistent with previous reports [16].

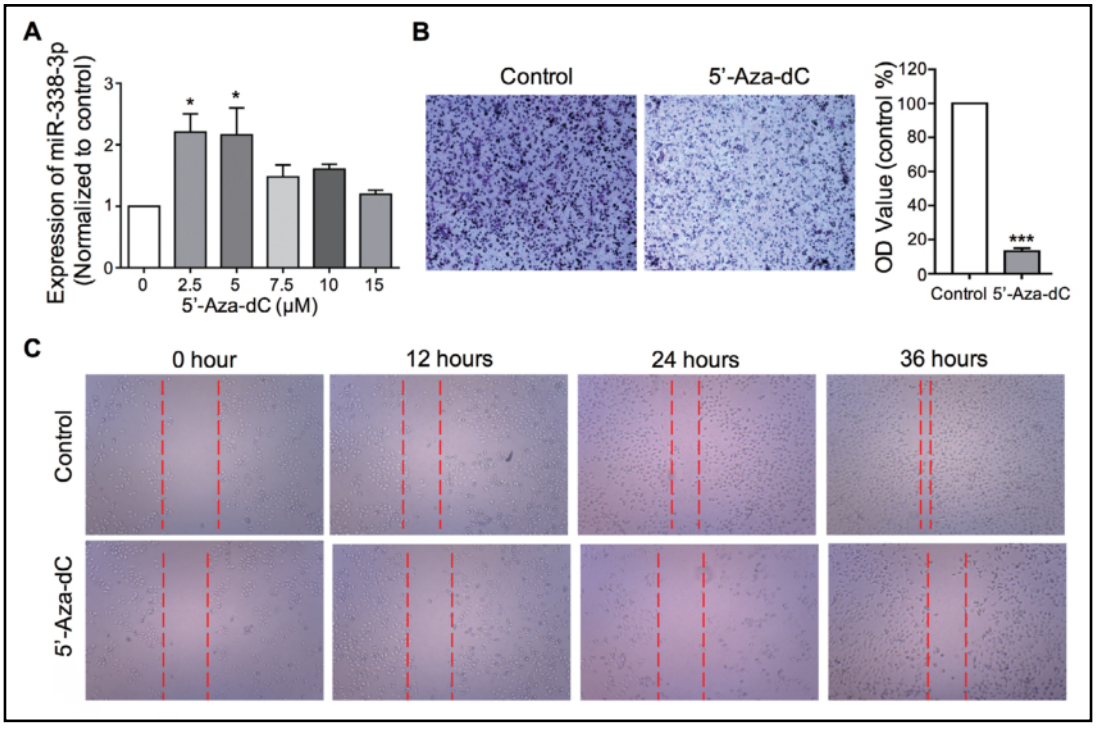

Fig. 3. Inhibition of GC cell invasion and migration after 5'-Aza-dC treatment (A) qRT-PCR analysis of miR-338-3p expression in BGC-823 cells after 5'-Aza-dC treatment and normalized against an endogenous control (U6 RNA). Data were analyzed using a ΔΔCt approach. (B) Tumor cell invasion assay. BGC-823 cells were treated with 2.5 μM 5'-Aza-dC. Then, the treated cells were seeded into Transwell upper chambers for the cell invasion assay. Cells were transferred to the reverse side of the filter (left panel) and stained with 1% crystal violet for OD value measurements (right panel). (C) Wound healing assay. BGC-823 cells were treated with 5'-Aza-dCas described above. Photographs were taken every 12 hours and the remaining unhealed gap was marked. All data are shown as the mean ± SD for 3 independent experiments (*P<0.05, ***P<0.001).

miR-338-3p suppresses metastasis by targeting the Hhat-MMP signaling pathway

miRNAs were involved in the regulation of cancer progress by targeting multiple genes. In this study, from bioinformatics databases, we identified a metastasis-related target gene with a well-matched 3'-UTR, Hhat, which has been proven to promote metastasis and lymphangiogenesis in GC [17]. To validate this hypothesis, we employed a dual-luciferase reporter system as mentioned above (Fig. 6A), which resulted in an assured interaction between miR-338-3p and Hhat (Fig. 6B). Additionally, we found it was inversely correlated with miR-338-3p (Fig. 6C). To test the effect of Hhat on cell metastasis, we used shRNA to knockdown its expression in BGC-823 cells (Fig. 6D), which resulted in a considerable decrease in wound-healing capacity (Fig. 6E) and cell migration (Fig. 6F). After carrying out a literature review, we subsequently examined whether MMP was involved in Hhat-mediated cell metastasis regulation. Western blots showed that both MMP-2 and MMP-9 expression were completely abolished by the inhibition of Hhat with miR-338-3p and shRNA (Fig. 6G), which is in accordance with the results of a previous study on liver cancer cells [18]. Taken together, these findings suggest that miR-338-3p could inhibit cell metastasis through Hhat-mediated MMP-2 and MMP-9 in GC cells.

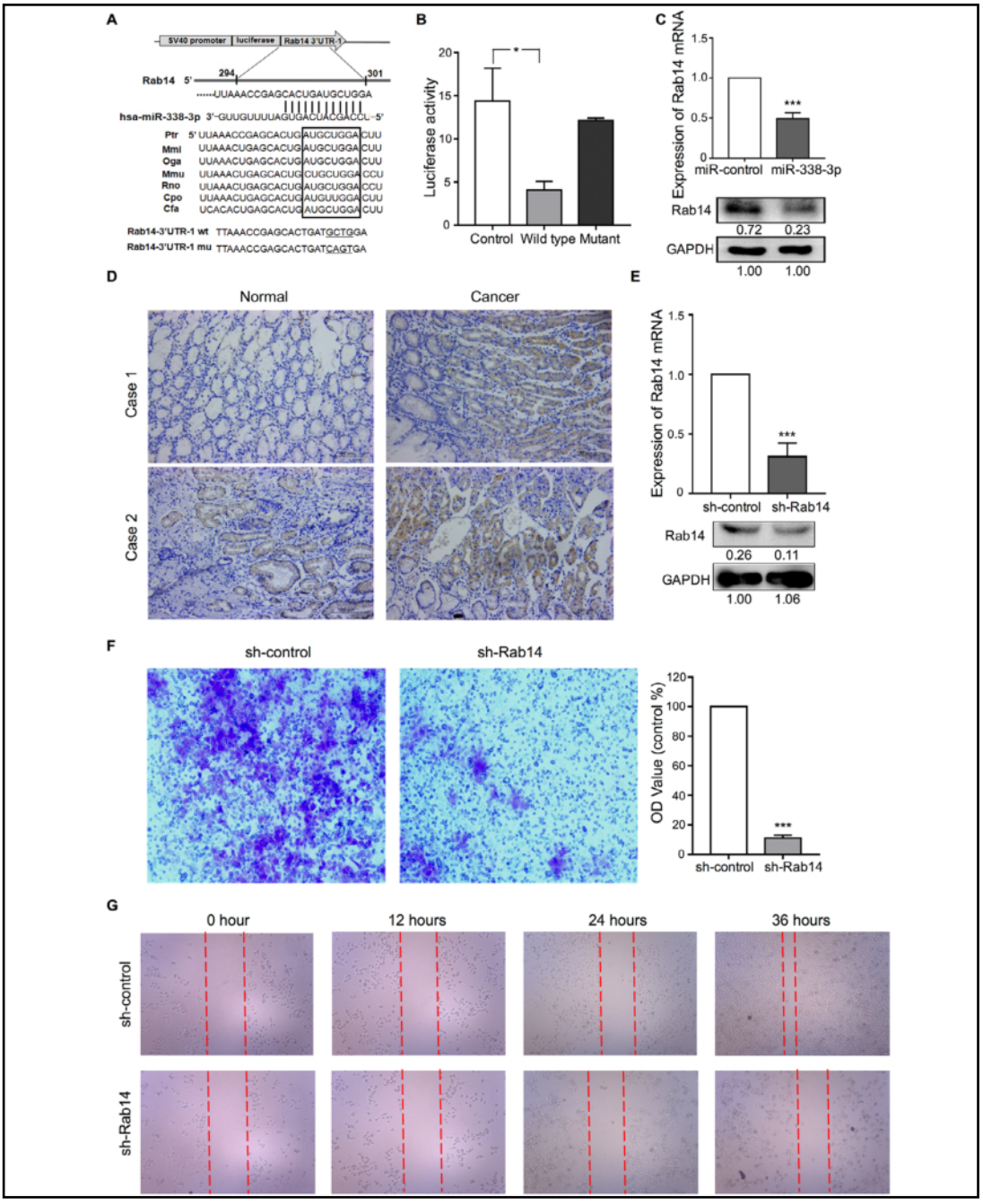

Fig. 4. Rab14 is experimentally validated as a direct target of miR-338-3p in GC cells. (A) miR-338-3p is highly conserved across species and binding sites within the seeded region sequence in the 3'-UTR of human Rab14. (B) Luciferase assay in HEK-293 cells. pLUC-Rab14_WT vector or pLUC-Rab14_MT was co-transfected with miR-338-3p. The relative repression of luciferase expression was standardized to the β-gal signal. The luciferase activity in the pLUC-Rab14_WT group denoted a statistically significant decrease following ectopic expression of miR-338-3p. (C) Rab14 mRNA (upper) and protein (lower) expression level measured by qRT-PCR and western blot analysis after transfection with miR-338-3p vector. GAPDH was used as a housekeeping control. (D) Expression of Rab14 determined by immunohistochemistry assay in randomly selected GC tissues and their corresponding normal tissues. (E) Rab14 mRNA (upper) and protein (lower) expression levels were measured to confirm the knock-down efficiency after transfection with shRNA targeting Rab14. (F/G) Cell invasion and wound healing assays were performed to reveal the suppression of cell metastasis after silencing of Rab14. (*P<0.05, ***P<0.001).

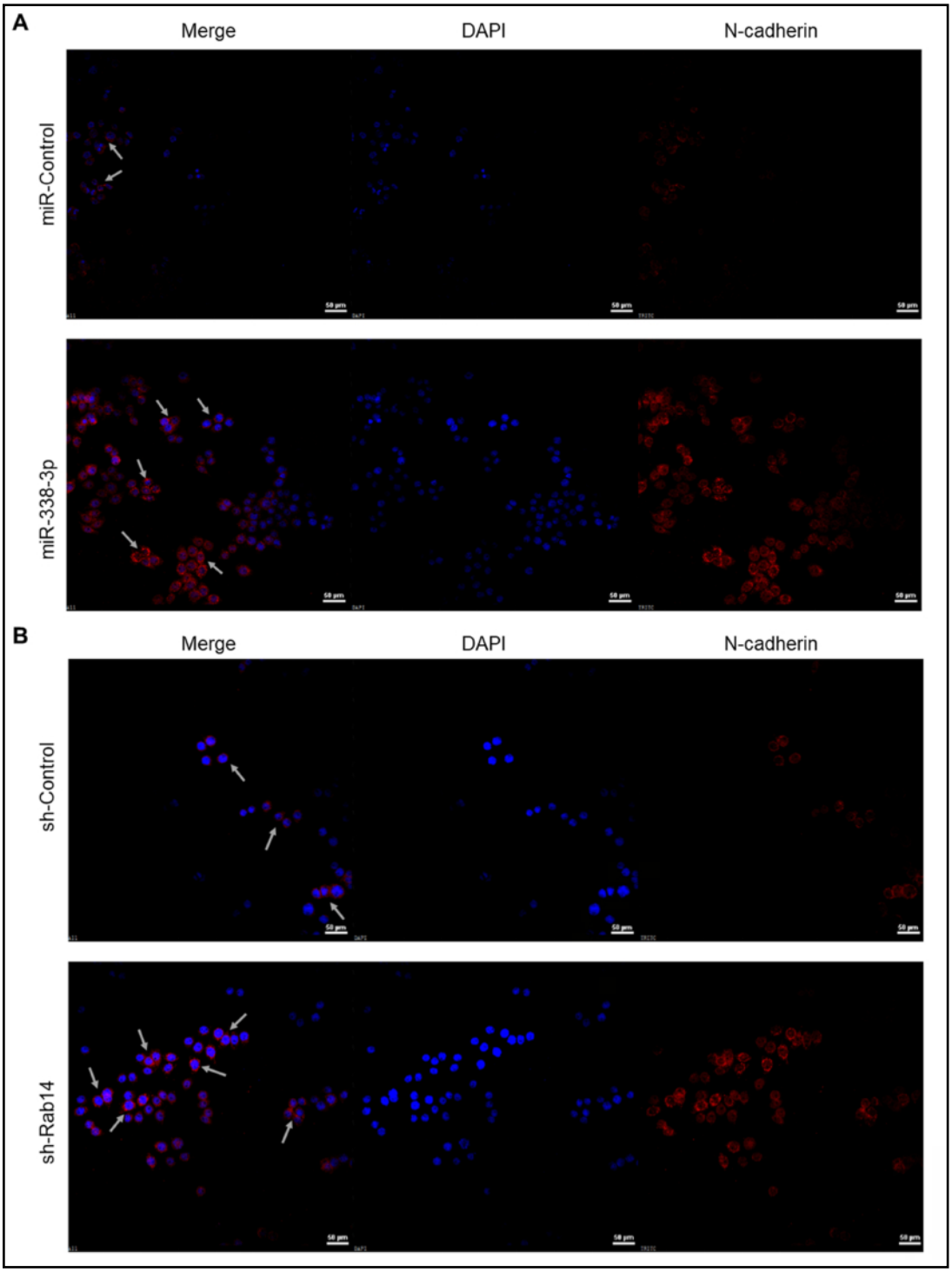

Fig. 5. N-Cadherin accumulation at cell-cell junctions in Rab14-silenced cells. BGC-823 cells were treated with miR-338-3p (A) and sh-Rab14 (B) to silence Rab14, fixed, and then stained with DAPI and N-cadherin antibodies. White arrows mark the regions of N-cadherin accumulation. The scale bar indicates 50 μm in all images.

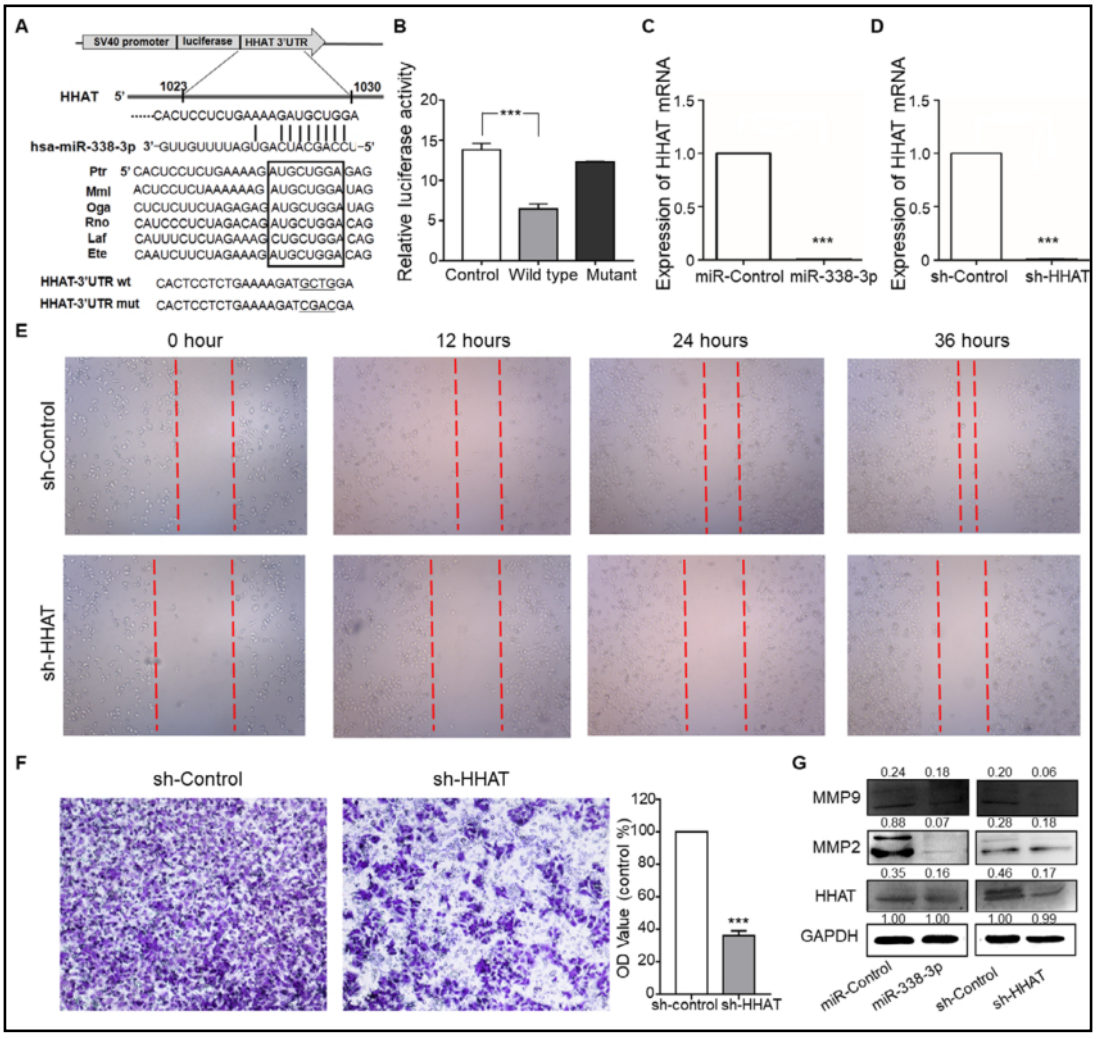

Fig. 6. miR-338-3p suppresses metastasis by targeting the Hhat-MMP signaling pathway. (A) miR-338-3p is highly conserved across species and binding sites within the seeded region sequence in the 3′-UTR of human HHAT. (B) Luciferase assay in HEK-293 cells as described above. Luciferase activity in pLUC-HHAT_WT group denoted a statistically significant decrease following ectopic expression of miR-338-3p. (C/D) HHAT mRNA expression level measured by qRT-PCR after transfection with miR-338-3p vector or sh-HHAT. GAPDH was used as a housekeeping control. (E/F) Cell invasion and wound healing assays were performed to reveal the suppression of cell metastasis after silencing of HHAT. (G) Expression analysis for HHAT-regulated MMP proteins in BGC-823 cells after transfection with miR-338-3p or sh-HHAT by western blot analysis. GAPDH was used as a housekeeping control. (*P<0.05, ***P<0.001).

Discussion

The expression of miR-338-3p has been well-described in several tumor types, including hepatocellular carcinoma [19], ovarian epithelial carcinoma [20], lung cancer [21], colorectal carcinoma [22], and breast cancer [23], as well as GC [24, 25]. However, few studies have focused on the regulation of miR-338-3p expression, and the mechanism of miR-338-3p regulation has remained unclear until now. Previous studies have demonstrated that the silencing of primary transcripts by the CpG island promoter hypermethylation is one of the most common causes for the loss of tumor-suppressor miRNAs in human cancer [26]. For example, miR-145 is a well-known tumor suppressor that is down-regulated in many human cancers and which was found to undergo aberrant DNA methylation in its promoter [27].

Moreover, miR-199a is regulated by DNA methylation of the locus from which it is transcribed and the association between this downregulation and the aberrant DNA hypermethylation of its promoter has been described in GC [28]. Based on our previous study, we found that miR-338-3p expression was downregulated in both GC tissues and cells, and this downregulation is closely associated with hypermethylation in one of its CpG islands at the promoter region, which was also substantiated in Li et al.'s study using methylation-specific PCR [24].

The survival and prognosis of GC are poor partly because of relapse and metastasis. In this study, we found that downregulation of miR-338-3p is clinically associated with the Bormann stage. This stage is classified as advanced GC according to the Japanese Gastric Cancer Association [29], mainly based on endoscopic or gross morphologic appearance [30]. To extend our previous observation, we focused on the role of miR-338-3p in the regulation of migration and invasion, as well as gene expression, in GC. We discovered that enforced expression of miR-338-3p could suppress the migrative and invasive potential of GC cells. Consistently, this suppression also occurred after treatment with 5'-Aza-dC, accompanied with a restoration of miR-338-3p expression.

To understand the possible mechanisms underlying miR-338-3p-mediated suppression of migration and invasion, we used miRanda, PicTar, and TargetScan to predict potential targets of miR-338-3p. We identified Rab14, the final member of the Rab11 subfamily isolated from migrating cells [31]. Silencing Rab14 has been shown to result in increased N-cadherin levels at junctional complexes and cannot resolve cell-cell junctions in migrating cells [16]. The Rab family of small GTPase is highly involved in various aspects of membrane traffic control; for example, they function as molecular switches regulating vesicular transport in eukaryotic cells [32, 33]. Recently, Rab-GTPase-directed endocytic trafficking pathways have begun to emerge as key transport events required for the remodeling of cell adhesion and cellular junctions as well as migration [34, 35]. For example, Rab27 has been reported to be involved in exocytosis of endocrine cells and is associated with the invasive and metastatic potential of breast cancer, promoting the secretion of insulin-like growth factor-II [36]. Another study demonstrated that Rab27b controls vesicle exocytosis and releases important growth regulators into the tumor microenvironment, leading to regulation of invasive growth and metastasis in ER-positive human breast tumors [37]. In our study, we constructed dual-luciferase reporter systems to verify that Rab14 is targeted by miR-338-3p, and the forced expression of miR-338-3p reduced the expression of Rab14. Furthermore, we performed RNA interference to knock-down Rab14, and our findings showed that sh-Rab14 could also significantly inhibit the migration and invasion of GC cells. Subsequently, we used immunofluorescence microscopy to explore the location of N-cadherin and found that both enforced miR-338-3p and sh-Rab14 induced accumulation of N-cadherin at cell-cell junctional complexes, which explained their suppressive role on cell migration and invasion in GC cells. These results demonstrated that miR-338-3p could inhibit GC cell migration and invasion through targeting Rab14.

It is well-known that miRNAs can regulate hundreds of potential targets. We verified that Hhat is targeted by miR-338-3p using dual-luciferase reporter systems and RNA interference in this system. Hhat functions as a palmitoyl acyltransferase with specificity for *N*-palmitoylation of the Sonic Hedgehog (SHH) signaling pathway in COS-1 cells [38]. Activation of the sonic hedgehog signaling pathway can promote cell metastasis through the PI3K/AKT pathway, which will lead to MMP-9 activation in liver cancer [18] and GC [17]. The degradation of the basement membrane (BM) and the extracellular matrix (ECM) are critical events in tumor invasion and metastasis [39]. MMPs, especially MMP-2 and MMP-9, are the most important enzymes for BM and ECM degradation. Our results showed that both MMP-2 and MMP-9 expression decreased in GC cells transfected with miR-338-3p and sh-Hhat, respectively, which indicates that miR-338-3p could also suppress the migration and invasion of GC cells through Hhat-regulated MMP expression.

Conclusion

In conclusion, the present study demonstrates that miR-338-3p is frequently silenced by epigenetic hypermethylation in its promoter region. Functionally, miR-338-3p could inhibit the metastatic feature of GC cells such as migration and invasion *in vitro*. Moreover, we identified Rab14-mediated N-cadherin and the Hhat-MMP signaling pathway as key targets of miR-338-3p. These results enhance our understanding of the regulation and functions of miR-338-3p in GC progression and suggest that miR-338-3p could be used as a potential target for miR-based GC therapy.

Acknowledgements

This work was financially supported by National Natural Science Foundation of China (81660492), National Natural Science Foundation of China (81702765), China Postdoctoral Science Foundation (2016M602801), Shaanxi Province Innovative Talents Promotion Plan (2017KJXX-20), Shaanxi Province Postdoctoral Science Foundation (2016BSHEDZZ90) and the Fundamental Research Funds for the Central Universities (0811/1191320073).

Disclosure Statement

No potential conflicts of interest were disclosed.

References

1 Parkin DM, Bray F, Ferlay J, Pisani P: Global cancer statistics, 2002. CA: Cancer J Clin 2005;55:74-108.
2 Ishiguro H, Kimura M, Takeyama H: Role of microRNAs in gastric cancer. World J Gastroenterol 2014;20:5694.
3 Tsai KW, Wu CW, Hu LY, Li SC, Liao YL, Lai CH, Kao HW, Fang WL, Huang KH, Chan WC: Epigenetic regulation of miR-34b and miR-129 expression in gastric cancer. Int J Cancer 2011;129:2600-2610.
4 Huang YW, Liu JC, Deatherage DE, Luo J, Mutch DG, Goodfellow PJ, Miller DS, Huang TH: Epigenetic repression of microRNA-129-2 leads to overexpression of SOX4 oncogene in endometrial cancer. Cancer Res 2009;69:9038-9046.
5 Kim K, Lee HC, Park JL, Kim M, Kim SY, Noh SM, Song KS, Kim JC, Kim YS: Epigenetic regulation of microRNA-10b and targeting of oncogenic MAPRE1 in gastric cancer. Epigenetics 2011;6:740-751.
6 Guo B, Liu L, Yao J, Ma R, Chang D, Li Z, Song T, Huang C: miR-338-3p suppresses gastric cancer progression through a PTEN-AKT axis by targeting P-REX2a. Mol Cancer Res 2014;12:313-321.
7 Ma L, Teruya-Feldstein J, Weinberg RA: Tumour invasion and metastasis initiated by microRNA-10b in breast cancer. Nature 2007;449:682-688.
8 Huang Q, Gumireddy K, Schrier M, le Sage C, Nagel R, Nair S, Egan DA, Li A, Huang G, Klein-Szanto AJ: The microRNAs miR-373 and miR-520c promote tumour invasion and metastasis. Nature Cell Biol 2008;10:202-210.
9 Baranwal S, Alahari SK: miRNA control of tumor cell invasion and metastasis. Int J Cancer 2010;126:1283-1290.
10 Tie J, Pan Y, Zhao L, Wu K, Liu J, Sun S, Guo X, Wang B, Gang Y, Zhang Y: MiR-218 inhibits invasion and metastasis of gastric cancer by targeting the Robo1 receptor. PLoS Genet 2010;6:e1000879.
11 Li X, Zhang Y, Shi Y, Dong G, Liang J, Han Y, Wang X, Zhao Q, Ding J, Wu K: MicroRNA-107, an oncogene microRNA that regulates tumour invasion and metastasis by targeting DICER1 in gastric cancer. J Cell Mol Med 2011;15:1887.
12 Song G, Zeng H, Li J, Xiao L, He Y, Tang Y, Li Y: miR-199a regulates the tumor suppressor mitogen-activated protein kinase kinase kinase 11 in gastric cancer. Biol Pharm Bull 2010;33:1822-1827.

13 An JY, Kang TH, Choi MG, Noh JH, Sohn TS, Kim S: Borrmann type IV: an independent prognostic factor for survival in gastric cancer. J Gastrointest Surg 2008;12:1364-1369.
14 Guo B, Wang W, Zhao Z, Li Q, Zhou K, Zhao L, Wang L, Yang J, Huang C: Rab14 Act as Oncogene and Induce Proliferation of Gastric Cancer Cells via AKT Signaling Pathway. Plos One 2017;12:e0170620.
15 Junutula JR, De Maziére AM, Peden AA, Ervin KE, Advani RJ, van Dijk SM, Klumperman J, Scheller RH: Rab14 is involved in membrane trafficking between the Golgi complex and endosomes. Mol Biol Cell 2004;15:2218.
16 Linford A, Yoshimura S, Nunes Bastos R, Langemeyer L, Gerondopoulos A, Rigden DJ, Barr FA: Rab14 and its exchange factor FAM116 link endocytic recycling and adherens junction stability in migrating cells. Dev Cell 2012;22:952-966.
17 Yoo YA, Kang MH, Lee HJ, Kim BH, Park JK, Kim HK, Kim JS, Oh SC: Sonic hedgehog pathway promotes metastasis and lymphangiogenesis via activation of Akt, EMT, and MMP-9 pathway in gastric cancer. Cancer Res 2011;71:7061-7070.
18 Chen JS, Huang XH, Wang Q, Huang JQ, Zhang LJ, Chen XL, Lei J, Cheng ZX: Sonic hedgehog signaling pathway induces cell migration and invasion through focal adhesion kinase/AKT signaling-mediated activation of matrix metalloproteinase (MMP)-2 and MMP-9 in liver cancer. Carcinogenesis 2013;34:10.
19 Huang XH, Chen JS, Wang Q, Chen XL, Wen L, Chen LZ, Bi J, Zhang LJ, Su Q, Zeng WT: miR-338-3p suppresses invasion of liver cancer cell by targeting smoothened. J Pathol 2011;225:463-472.
20 Wen C, Liu X, Ma H, Zhang W, Li H: miR-338-3p suppresses tumor growth of ovarian epithelial carcinoma by targeting Runx2. Int J Oncol 2015;46:2277-2285.
21 Li Y, Chen P, Zu L, Liu B, Wang M, Zhou Q: MicroRNA-338-3p suppresses metastasis of lung cancer cells by targeting the EMT regulator Sox4. Am J Cancer Res 2016;6:127.
22 Xue Q, Sun K, Deng HJ, Lei ST, Dong JQ, Li GX: MicroRNA-338-3p inhibits colorectal carcinoma cell invasion and migration by targeting smoothened. Japan J Clin Oncol 2014;44:13-21.
23 Jin Y, Zhao M, Xie Q, Zhang H, Wang Q, Ma Q: MicroRNA-338-3p functions as tumor suppressor in breast cancer by targeting SOX4. Int J Oncol 2015;47:1594.
24 Li P, Chen X, Su L, Li C, Zhi Q, Yu B, Sheng H, Wang J, Feng R, Cai Q: Epigenetic silencing of miR-338-3p contributes to tumorigenicity in gastric cancer by targeting SSX2IP. PLoS One 2013;8:e66782.
25 Chen JT, Yao KH, Hua L, Zhang LP, Wang CY, Zhang JJ: MiR-338-3p inhibits the proliferation and migration of gastric cancer cells by targeting ADAM17. Int J Clin Exp Pathol 2015;8:10922-10928.
26 Saxonov S, Berg P, Brutlag DL: A genome-wide analysis of CpG dinucleotides in the human genome distinguishes two distinct classes of promoters. Proc Natl Acad Sci U S A 2006;103:1412-1417.
27 Suh SO, Chen Y, Zaman MS, Hirata H, Yamamura S, Shahryari V, Liu J, Tabatabai ZL, Kakar S, Deng G: MicroRNA-145 is regulated by DNA methylation and p53 gene mutation in prostate cancer. Carcinogenesis 2011;32:772.
28 Ueda T, Volinia S, Okumura H, Shimizu M, Taccioli C, Rossi S, Alder H, Liu CG, Oue N, Yasui W: Relation between microRNA expression and progression and prognosis of gastric cancer: a microRNA expression analysis. Lancet Oncology 2010;11:136-146.
29 Kajitani T: The general rules for the gastric cancer study in surgery and pathology. Japan J Surgery 1981;11:140-145.
30 Sendler A, Dittler HJ, Feussner H, Nekarda H, Bollschweiler E, Fink U, Helmberger H, Hofler H, Siewert JR: Preoperative staging of gastric cancer as precondition for multimodal treatment. World J Surg 1995;19:501-508.
31 Howes MT, Kirkham M, Riches J, Cortese K, Walser PJ, Simpson F, Hill MM, Jones A, Lundmark R, Lindsay MR: Clathrin-independent carriers form a high capacity endocytic sorting system at the leading edge of migrating cells. J Cell Biol 2010;190:675-691.
32 Pereira-Leal JB, Seabra MC: Evolution of the Rab family of small GTP-binding proteins. J Mol Biol 2001;313:889-901.
33 Deneka M, Neeft M, van der Sluijs P: Regulation of membrane transport by rab GTPases. Crit Rev Biochem Mol Biol 2003;38:121-142.
34 Baum B, Georgiou M: Dynamics of adherens junctions in epithelial establishment, maintenance, and remodeling. J Cell Biol 2011;192:907-917.
35 Caswell PT, Vadrevu S, Norman JC: Integrins: masters and slaves of endocytic transport. Nature Rev Mol Cell Biol 2009;10:843-853.

36 Wang JS, Wang FB, Zhang QG, Shen ZZ, Shao ZM: Enhanced expression of Rab27A gene by breast cancer cells promoting invasiveness and the metastasis potential by secretion of insulin-like growth factor-II. Mol Cancer Res 2008;6:372-382.

37 Hendrix A, Maynard D, Pauwels P, Braems G, Denys H, Van den Broecke R, Lambert J, Van Belle S, Cocquyt V, Gespach C: Effect of the secretory small GTPase Rab27B on breast cancer growth, invasion, and metastasis. J Natl Cancer Inst 2010;102:866-880.

38 Buglino JA, Resh MD: Hhat is a palmitoylacyltransferase with specificity for N-palmitoylation of Sonic Hedgehog. J Biol Chem 2008;283:22076-22088.

39 Rowe RG, Weiss SJ: Navigating ECM Barriers at the Invasive Front: The Cancer Cell–Stroma Interface. Annu Rev Cell Dev Biol 2009;25:567-595.